Spectrochimica Acta Part A: Molecular and Biomolecular Spectroscopy 245 (2021) 118907

Contents lists available at ScienceDirect

Spectrochimica Acta Part A: Molecular and Biomolecular Spectroscopy

journal homepage: www.elsevier.com/locate/saa

Structurally-thrifty and visible-absorbing fluorophores

Xiao Luo [a,b], Yan Chen [a], Yanchun Li [a], Zhenglong Sun [c,*], Weihong Zhu [d,*], Xuhong Qian [a], Youjun Yang [a,*]

[a] State Key Laboratory of Bioreactor Engineering, School of Pharmacy, East China University of Science and Technology, Shanghai 200237, China
[b] School of Chemistry and Molecular Engineering, East China Normal University, Shanghai 200241, China
[c] Suzhou Institute of Biomedical Engineering and Technology (SIBET), Chinese Academy of Sciences, Suzhou, Jiangsu 215163, China
[d] Key Laboratory for Advanced Materials, Joint International Research Laboratory of Precision Chemistry and Molecular Engineering, Feringa Nobel Prize Scientist Joint Research Center, Institute of Fine Chemicals, School of Chemistry and Molecular Engineering, East China University of Science and Technology, Shanghai 200237, China

ARTICLE INFO

Article history:
Received 28 July 2020
Received in revised form 13 August 2020
Accepted 29 August 2020
Available online 4 September 2020

Keywords:
Structurally-thrifty
D′D-π-A
Visible-absorbing
Green emission
Cell imaging

ABSTRACT

Fluorophores with a minimal push-pull backbone are actively pursued due to their potentials in biological labelling. Herein a series of structurally-thrifty and visible-absorbing fluorophores (**SDX**s) were successfully constructed following the D′D-π-A design strategy, in which a secondary donor (D′) was introduced in conjugation with the donor (D) to enhance its electron donating capability. For a very small scaffold, **SDX**s exhibit a surprisingly long-wavelength absorption band in the visible spectral range (λ_{abs} = 420 nm) and a strong green fluorescence emission (λ_{em} = 530 nm) with a fluorescence quantum yield up to 0.84. Notably, fluorescence of **SDX**s was quenched in hydrogen-bonding solvents, e.g. MeOH and H_2O. This phenomenon renders **SDX**s feasibility for imaging of cellular non-hydrogen-bonding microenvironment, as demonstrated with BEAS-2B cells. These results proved that the D′D-π-A is a powerful design strategy to construct novel structurally-thrifty fluorophores.

1. Introduction

Fluorescent dyes are particularly suitable for biological imaging due to its sensitivity for detection, versatility for manipulation, and feasibility for complex matrix [1–3]. Over the years, they have become indispensable for a variety of basic, translational and clinical applications [4–6]. For a fluorescent dye to find practical applications, it should exhibit localization-specificity toward the structure-of-interest in the complex biological matrix. Target-specificity in biological labelling is typically achieved harnessing preferential solubility, dipole-dipole interaction, antibody-antigen interaction, ligand-receptor interaction, genetic labelling, or covalent bond modification [7–9]. Recently, metabolic labelling of oligosaccharides with unnatural saccharides or proteins with unnatural amino acids by the cell biosynthesis machinery has attracted tremendous attention [10,11]. A high degree of structural similarity to the native substrate is necessary to bypass the specificity of enzyme. Even the relatively small ones of the existing classic fluorophores, e.g. coumarin, NBD, dansyl, etc., are still not small enough, not to mention naphthalimides, BODIPY, xanthenes, cyanines, etc. [12,13]. While the structure of a dye should be kept small, its absorbing wavelength should be long enough, e.g. the visible spectral region, not to readily induce injuries to biological molecules [14]. Therefore, it is our goal to develop small molecules absorbing and emitting beyond 400 nm (Fig. 1).

The UV–Vis absorption of a fluorochrome is the result of HOMO-LUMO electronic transition, i.e. π-π* and n-π* (Fig. 1). Since n-π* is typically of low absorptivity due to its spin-forbidden nature, it is not considered further [15]. The Lewis structure of a given fluorochrome with a π-π* transition typically exhibits a theme of D-π-A. To render long-wavelength absorption for a D-π-A scaffold, the following three approaches may be adopted, enhancing the electron-donating/withdrawing capability of the donor (D)/acceptor (A), respectively, elongating the π backbone in between, and substituting the π backbone to destabilize the ground state (S_0) or stabilize the first singlet excited state (S_1) following the perturbation theory [16,17]. Since it is the goal of this manuscript to develop structurally thrifty dyes, we wish to keep the π backbone as small as possible, i.e. an ethylene unit. In this case, a viable approach to red-shift the absorption maxima is to make the donor more donating and the acceptor more withdrawing [18]. A secondary donor (D′) in conjugation destabilizes the lone-pair of D and renders D more electron-donating. Analogously, a secondary acceptor (A′) in conjugation destabilizes the empty orbital of A and renders A more electron-withdrawing [19]. Not surprisingly, the generic structure of D′-π-D-π-A-π-A′ has been proposed as a guideline to develop dyes exhibiting an even longer-wavelength absorption than what D-π-A could possibly render [20,21]. However, a D′-π-D-π-A-π-A′ type dye will not be structurally thrifty, without a doubt. We were further

* Corresponding authors.
E-mail addresses: sunzhl@sibet.ac.cn (Z. Sun), weihongzhu@ecust.edu.cn (W. Zhu), youjunyang@ecust.edu.cn (Y. Yang).

https://doi.org/10.1016/j.saa.2020.118907
1386-1425/

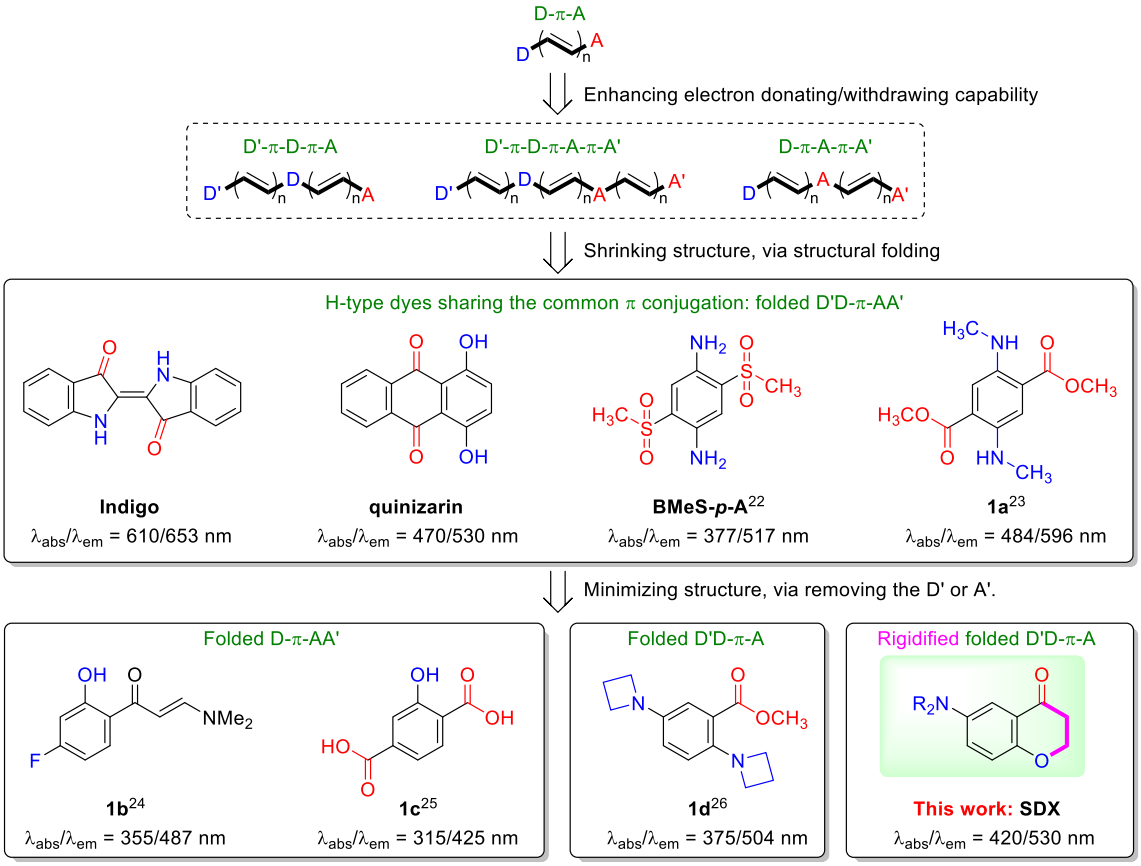

Fig. 1. Folded D′D-π-A: the optimal design strategies of developing structurally-thrifty fluorophores with long absorption and emission wavelength.

inspired by the structural features of a special class of fluorophores, commonly referred to as H-chromophores [22]. In such dyes, the π scaffold of the D-π-A is also the π scaffold of the D′-π-D and/or A′-π-A. We call such a design principle, folded D′D-π-AA′. The most notable dye of this class is indigo [23], a red-absorbing dye with a rather small scaffold, quinone dyes [24], and many single-benzene fluorophores with two donors at C-1,4 and two acceptors at C-2,5, i.e. D′D-π-AA′ [25,26], are also dyes of this type. We wish to further shrink the scaffold of folded D′D-π-AA′ to folded D-π-AA′ [27,28] or folded D′D-π-A [29], by eliminating a D′ or a A′ group. While minimizing the structure, we also expect that the maximal absorption wavelength should be kept longer than 400 nm, the light of which spectral region is comparatively less absorbed and less toxic to the biological macromolecules than the light of shorter spectral region.

Herein, we developed a series of structurally-thrifty fluorophores (**SDX**) utilizing a rigidified folded D′D-π-A design strategy. Rigidification mandates coplanarity of the D and A, enhances the electron-delocalization, and is the highlight of this approach compared to the literature analogous. **SDX**s exhibit visible absorption and fluorescence emission maxima. **SDX**s showed high fluorescent quantum yields, among which **SDX4** possessed a reddest absorption wavelength of ca. 420 nm and emitted strong green fluorescence with a large Stokes shift over 100 nm. The fluorescence emission of **SDX**s was highly sensitive to hydrogen bonding. Finally, **SDX**s were feasible live cell imaging.

2. Experimental

2.1. Material and instruments

All chemical regents and solvents were purchased from commercial suppliers and were used without further purification. The ^{1}H NMR and ^{13}C NMR spectra were collected on a Bruker AV-400 spectrometer. HRMS spectra were acquired on a Micromass GCT spectrometer. Absorption spectra were collected by a SHIMADZU UV-2600 UV–vis spectrophotometer. Fluorescence excitation and emission spectra were collected in a PTI-QM4 steady-stead fluorimeter with a 75 W Xenon arc-lamp and a model 810 PMT. The voltage of PMT was 950 V. The excitation and emission slits were set to 2 nm.

2.2. Synthesis of 8-nitrochroman-4-one (*2*) and 6-nitrochroman-4-one (*3*)

To a 25 mL round bottomed flask was added 4-chromanone (**1**, 5.0 g, 1 equiv., 33.97 mmol) and concentrated sulfuric acid (10 mL). The mixture was cooled to 0 °C, and then a mixture of concentrated sulfuric acid (2 mL) and concentrated nitric acid (2.25 mL, 1.00 equiv., 33.97 mmol) was added dropwise over 15 min. The resultant solution was stirred at 25 °C for 30 min before poured into ice water. Light yellow precipitates were collected via a suction filtration and then purified by a flash column using a mixture of petroleum ether and ethyl acetate [5:1, v/v] as an eluent to afford **2** [30] (1.83 g, 28%) and **3** (3.98 g, 61%) as white solid. Compound **2**: ^{1}H NMR (400 MHz, $CDCl_3$): δ 8.19 (dd, J = 7.8, 1.8 Hz, 1H), 8.11 (dd, J = 8.0, 1.8 Hz, 1H), 7.14 (t, J = 7.9 Hz, 1H), 4.73 (t, J = 6.5 Hz, 2H), 2.96 (t, J = 6.5 Hz, 2H); EI-MS (m/z): [M] calcd. for $C_9H_7NO_4$, 193.0375; found 193.0376. Compound **3**: ^{1}H NMR (400 MHz, $CDCl_3$): δ 8.74 (d, J = 2.8 Hz, 1H), 8.30 (dd, J = 9.1, 2.9 Hz, 1H), 7.10 (d, J = 9.1 Hz, 1H), 4.66 (t, J = 6.5 Hz, 2H), 2.89 (t, J = 6.5 Hz, 2H); ^{13}C NMR (101 MHz, $CDCl_3$) δ 189.7, 165.8, 142.1, 130.3, 123.8, 120.8, 119.4, 67.7, 37.2; EI-MS (m/z): [M] calcd. for $C_9H_7NO_4$, 193.0375; found 193.0374.

2.3. Synthesis of 8-aminochroman-4-one (*SDX1*)

Compound **2** (1 g, 1 equiv., 5.18 mmol) was dissolved in 20 mL of methanol, and Pd/C (100 mg) was added. The suspension was

deoxygenated and stirred under a hydrogen atmosphere (balloon) for 6 h at 25 °C. Powder of Pd/C was removed by filtration. The organic solvent in the filtrate was removed under reduced pressure to yield a yellow solid ***SDX1*** (778 mg) in a 92% yield and used without further purification. ^{1}H NMR (400 MHz, $CDCl_3$): δ 7.30 (ddd, J = 7.7, 1.6, 0.9 Hz, 1H), 6.90–6.80 (m, 2H), 4.57 (td, J = 6.4, 0.64 Hz, 2H), 2.81 (td, J = 6.4, 0.64 Hz, 2H); ^{13}C NMR (101 MHz, $CDCl_3$): δ 192.2, 150.0, 136.2, 121.4, 120.2, 116.1, 67.4, 38.0; EI-MS (m/z): [M] calcd. for $C_9H_9NO_2$, 163.0633; found 163.0634.

2.4. Synthesis of 6-aminochroman-4-one (*SDX2*)

Compound **3** (1 g, 1 equiv., 5.18 mmol) was dissolved in 20 mL of methanol, and Pd/C (100 mg) was added. The suspension was deoxygenated and stirred under a hydrogen atmosphere (balloon) for 6 h at 25 °C. Powder of Pd/C was removed by filtration. The organic solvent in the filtrate was removed under reduced pressure to yield a yellow solid **SDX2** (811 mg) in a 96% yield and used without further purification. ^{1}H NMR (400 MHz, $CDCl_3$): δ 7.16 (d, J = 2.9 Hz, 1H), 6.88 (dd, J = 8.7, 2.9 Hz, 1H), 6.81 (d, J = 8.7 Hz, 1H), 4.45 (t, J = 6.4 Hz, 2H), 3.55 (s, 2H), 2.76 (t, J = 6.4 Hz, 2H); ^{13}C NMR (101 MHz, $CDCl_3$): δ 192.4, 155.5, 140.6, 124.6, 121.7, 118.8, 111.2, 67.1, 38.1, 29.8; EI-MS (m/z): [M] calcd. for $C_9H_9NO_2$, 163.0633; found 163.0631.

2.5. Synthesis of 8-(diethylamino)chroman-4-one (*SDX3*)

SDX1 (500 mg, 1 equiv., 3.06 mmol), EtI (1.00 g, 2.1 equiv., 6.43 mmol), Na_2CO_3 (324 mg, 1 equiv., 3.06 mmol) and anhydrous acetonitrile (30 mL) were added into a 100 mL flask. The resulting mixture was heated to 80 °C with rigorous stirring for 10 h before being cooled to room temperature. Solid materials filtered off using a Celite cake under reduced pressure to give the crude product as a dark brown liquid, which was purified by a flash column using a mixture of petroleum ether and EtOAc [20:1, v/v] as an eluent to afford **SDX3** (624 mg) as a light yellow liquid in a 93% yield. ^{1}H NMR (400 MHz, $CDCl_3$): δ 7.14 (d, J = 3.2 Hz, 1H), 6.95 (dd, J = 9.1, 3.2 Hz, 1H), 6.86 (d, J = 9.0 Hz, 1H), 4.46 (t, J = 6.5 Hz, 2H), 3.30 (q, J = 7.1 Hz, 4H), 2.77 (t, J = 6.5 Hz, 2H), 1.11 (t, J = 7.1 Hz, 6H). ^{13}C NMR (101 MHz, $CDCl_3$): δ 192.8, 153.8, 143.1, 122.7, 121.6, 118.6, 108.7, 67.1, 44.9, 38.3, 12.5. EI-MS (m/z): [M] calcd. for $C_{13}H_{17}NO_2$, 219.1259; found 219.1258.

2.6. Synthesis of 6-(diethylamino)chroman-4-one (*SDX4*)

SDX2 (500 mg, 1 equiv., 3.06 mmol), EtI (1.00 g, 2.1 equiv., 6.43 mmol), Na_2CO_3 (324 mg, 1 equiv., 3.06 mmol) and anhydrous acetonitrile (30 mL) were added into a 100 mL flask. The resulting mixture was heated to 80 °C with rigorous stirring for 10 h before being cooled to room temperature. Solid materials filtered off using a Celite cake under reduced pressure to give the crude product as a dark brown liquid, which was purified by a flash column using a mixture of petroleum ether and EtOAc [20:1, v/v] as an eluent to afford **SDX4** (618 mg) as a light yellow liquid in a 93% yield. ^{1}H NMR (400 MHz, $CDCl_3$): δ 7.57 (dd, J = 7.9, 1.6 Hz, 1H), 7.11 (dd, J = 7.8, 1.6 Hz, 1H), 6.94 (t, J = 7.8 Hz, 1H), 4.59 (t, J = 6.4 Hz, 2H), 3.17 (d, J = 7.1 Hz, 4H), 2.81 (t, J = 6.4 Hz, 2H), 1.04 (t, J = 7.1 Hz, 6H). ^{13}C NMR (101 MHz, $CDCl_3$): δ 192.5, 156.5, 139.6, 127.4, 122.3, 120.8, 120.4, 67.2, 46.3, 37.8, 12.0. EI-MS (m/z): [M] calcd. for $C_{13}H_{17}NO_2$, 219.1259; found 219.1260.

2.7. Molar absorptivity and fluorescence quantum yields determinations

The DMSO solution of dyes at 10 mM were prepared and used as a stock for further preparation of dilute dye solutions. The absorption spectrum and the emission spectrum of the resulting solution with different dye concentration (in a 4 mL micro-fluorescence cuvette) were acquired until five sets of abs/em spectra with an absorbance below 0.1 were available. The abs/em spectra from these five sets were used to calculate the fluorescence quantum yields. The absorbance values were plotted against the dye concentration. The slope was calculated, which is the extinction coefficient of **SDX**. The relative fluorescence quantum yield of **SDX** in different solvents is calculated following a protocol [31]. A fluorescence quantum yield of 0.58 for the cation Coumarin 102 in EtOH was used as a reference to calculate the fluorescence quantum yields of **SDX** [32].

2.8. Cell culture and cell cytotoxicity

Human lung epithelial BEAS-2B cells were purchased from Cell Bank of Type Culture Collection of Chinese Academy of Sciences. BEAS-2B cells were maintained in Dulbecco's modified Eagle's medium (DMEM, Gibco) supplemented with 10% fetal bovine serum (FBS, Hyclone) and 1% penicillin-streptomycin. The cells were cultured in a humidified atmosphere of 5% CO_2/95% air at 37 °C and grown on 25 mm cover slips (Fisherbrand, 12-545-102) for 1–2 days to reach 70–90% confluency before use. Cytotoxicity study of **SDX2** was performed using Cell Counting Kit-8 (CCK-8) assay. BEAS-2B cells were grown to 70%–80% confluency before they were passaged. BEAS-2B cells were seeded into 96-well cell culture plate at 10^4/well, with 100 μL complete media for 24 h. A 10 mM stock solution of **SDX2** was diluted with complete medium to obtain different concentrations (0, 5, 10, 20, 30, 40 μM). The culture medium was carefully removed, and different concentrations of **SDX2** were added into each well. After incubation at 37 °C for 24 h, 10 μL Cell Counting Kit-8 (CCK-8) solution was added per well and the cells were incubated for another 2 h, then the absorbance at 450 nm was read by Microplate reader (Multiskan, Thermo Scientific, Waltham, MA, USA).

2.9. Fluorescent imaging

Confocal fluorescent images were recorded on Leica SP5 confocal microscope and 60× oil-immersion objective lens was used. BEAS-2B cells (approximately $5 * 10^4$) were seeded and cultured 24 h for adhesion in 15 mm glass-bottomed dishes. BEAS-2B cells were incubated with **SDX**s (20 μM) for 60 min and washed with PBS for three times to remove excess dyes. The excitation light source of is a 405 nm laser, and the emission wavelength collection range were 410–650 nm. The data obtained were analyzed and processed using Leica's own software and Image J.

3. Results and discussion

3.1. Molecular design and synthesis

Our approach to develop a structurally-thrifty dye with visible absorption and fluorescent emission wavelength was based on the design concept of D′D-π-A, i.e. further substituting a D-π-A scaffold with an electron donating group (D′) in conjugation with the electron donor (D). Such a secondary electron donor (D′) destabilizes the lone-pair of D and make D more electron-donating. The D-π-A scaffold to start with was 4-chromanone (**1**), in which the oxygen atom is the electron donor (D), the carbonyl group is the electron acceptor (A), and the double bond in between is the π conjugation system. Such a D-π-A scaffold is further rigidified by tethering the D and the A groups with an ethylene bridge, to increase the fluorescence quantum yield. A strongly electron-donating amino or diethylamino group was then introduced *ortho* or *para* to the electron-donating oxygen atom as the secondary electron donor.

SDXs were conveniently synthesized with high yields according to Scheme 1. Commercially available 4-chromanone (**1**) was nitrated with mixed acids of HNO_3 and H_2SO_4, resulting in a mixture of *ortho*- and *para*-nitration isomers, i.e. compound **2** and **3**, in a ca. 1:2 ratio. The mononitrated products (**2** and **3**) were reduced with catalytic hydrogenation to yield their corresponding amino derivatives (**SDX1** and

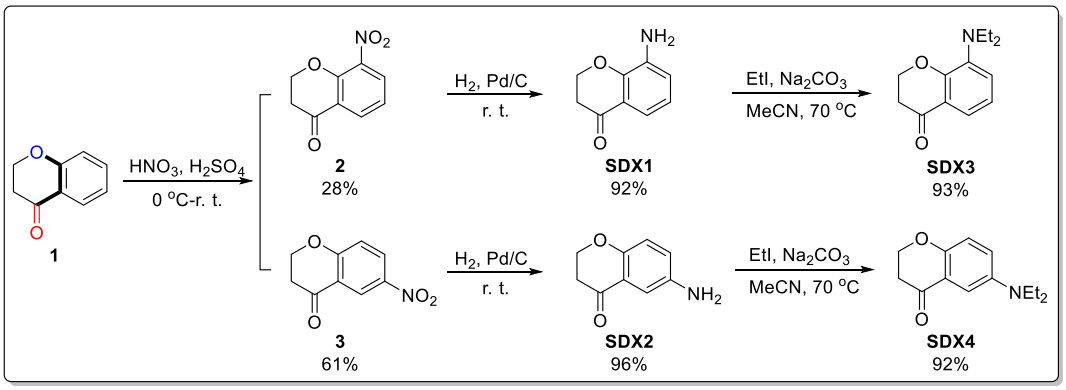

Scheme 1. Synthetic pathway of structurally-thrifty **SDX**s.

SDX2), respectively. The amino group of **SDX1** and **SDX2** was further alkylated with ethyl iodide to afford the **SDX3** and **SDX4**, respectively.

3.2. Spectroscopic properties of *SDX*s

The spectral properties of **SDX**s were studied in various organic solvents (Fig. 2 and Table 1). The maximal absorption wavelength of 4-chromanone (**1**) localizes at ca. 320 nm with an extinction coefficient of ca. 4.50×10^3 M^{-1} cm^{-1} (Fig. S1 and Table S1), in all six tested solvents of THF, CH_2Cl_2, acetone, EtOH, CH_3CN and DMSO. Compound **1** was not fluorescent in these solvents upon excitation at 320 nm. As expected, the absorption of **SDX1** or **SDX2** exhibited a notable bathochromic shift compared to **1**. For example, the absorption maximum of **SDX1** or **SDX2** in THF localizes at 360 and 380 nm, respectively, compared to the 320 nm of **1**. **SDX1** and **SDX2** did not exhibit a strong solvatochromism, exemplified by a ca. 10 nm bathochromic shift as the solvent polarities gradually increased from THF to CH_2Cl_2, acetone, EtOH, CH_3CN, and DMSO. Fortunately, **SDX1** and **SDX2** were fluorescent with a maximal emitting wavelength at 455 and 480 nm in THF upon excitation at 360 and 380 nm. And the fluorescence quantum yields

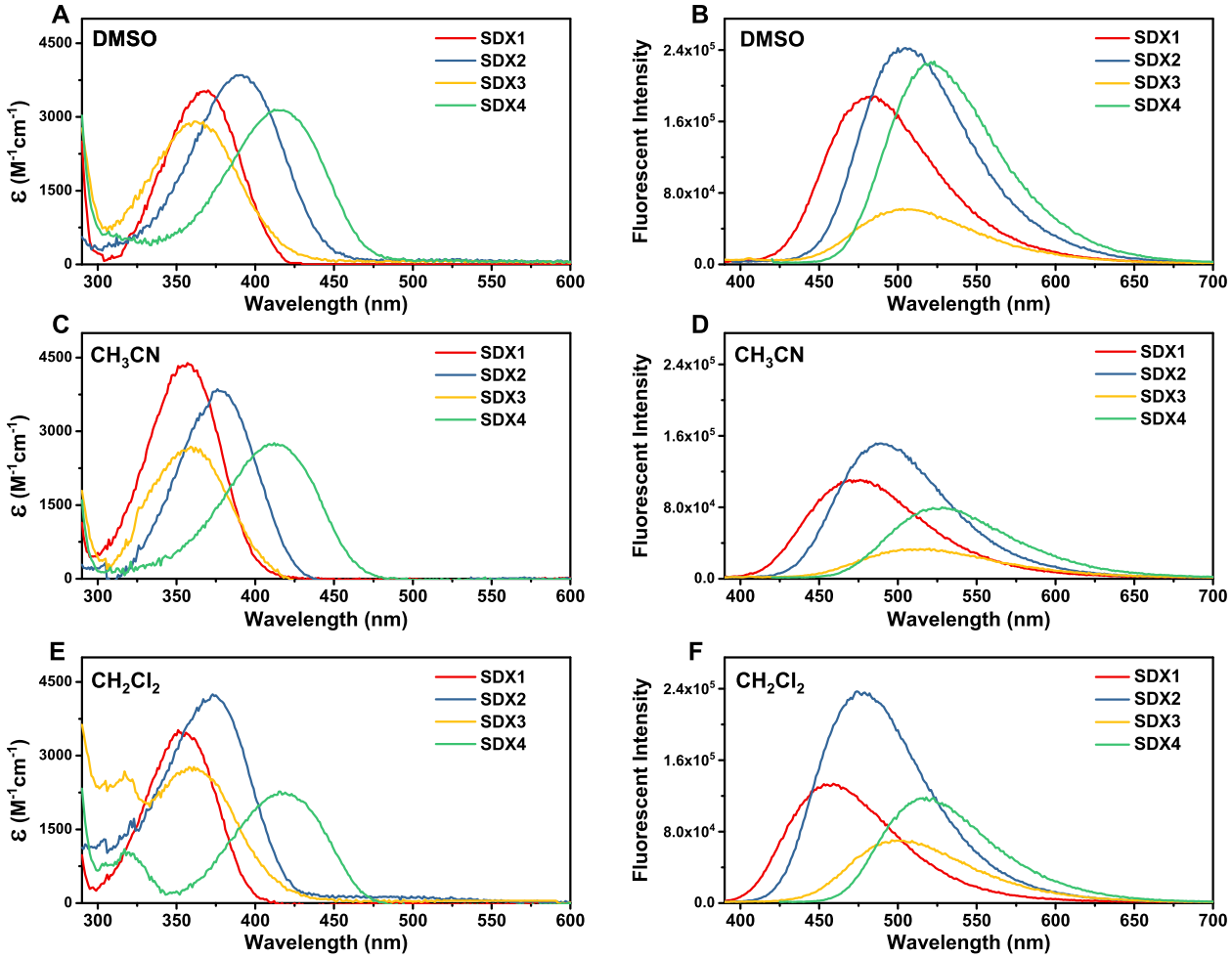

Fig. 2. The absorption and fluorescent emission spectra of **SDX**s in three solvents. In DMSO: (A) and (B). In CH_3CN: (C) and (D). In CH_2Cl_2: (E) and (F).

Table 1
The spectra properties of structurally-thrifty dyes (**SDX**) in different solvents.

Solvent	Compound	$\lambda_{abs.}^{max}$ [nm]	$\varepsilon/10^3$ [M^{-1} cm^{-1}]	$\lambda_{em.}^{max}$ [nm]	Stokes shift [nm]	Φ[a]
DMSO	**SDX1**	370	3.67	480	110	0.62
	SDX2	390	3.87	505	115	0.74
	SDX3	362	2.93	505	143	0.31
	SDX4	420	3.15	520	100	0.84
CH_3CN	**SDX1**	357	4.15	475	118	0.27
	SDX2	376	3.79	490	114	0.40
	SDX3	359	2.69	510	151	0.17
	SDX4	410	2.76	530	120	0.32
EtOH	**SDX1**	360	3.21	N.D.	N.A.	N.A.
	SDX2	375	3.77	N.D.	N.A.	N.A.
	SDX3	352	2.37	N.D.	N.A.	N.A.
	SDX4	420	2.35	N.D.	N.A.	N.A.
Acetone	**SDX1**	360	3.65	460	100	0.34
	SDX2	380	3.96	485	105	0.40
	SDX3	359	3.18	490	131	0.20
	SDX4	410	2.83	510	100	0.39
CH_2Cl_2	**SDX1**	353	3.63	460	107	0.42
	SDX2	375	4.23	475	100	0.59
	SDX3	361	2.77	500	139	0.31
	SDX4	415	2.27	520	105	0.56
THF	**SDX1**	360	3.51	455	95	0.43
	SDX2	380	4.10	480	100	0.48
	SDX3	354	2.87	470	116	0.34
	SDX4	410	3.07	495	85	0.53

[a] The quantum yields were determined with Coumarin 102 as the reference (Φ = 0.58 in EtOH). N.D.: Not determined. N.A.: Not applicable. (EtOH).

were 0.43 and 0.48, respectively. A bathochromic shift of the maximal emitting wavelength of ca. 25 nm was observed as the solvent varied from THF to DMSO. The fluorescence quantum yield was also mildly affectedly, exemplified by a increased fluorescence quantum yield of 0.62 and 0.74 in DMSO for **SDX1** and **SDX2**, respectively. This strongly supported the feasibility of our design principle of structurally-thrifty and visible absorbing/emitting fluorophores, i.e. D′D-π-A. The spectral wavelength of the *para*-substituted analog (**SDX2**) is consistently longer than the *ortho*-substituted (**SDX1**). Presumably, the amino group in **SDX1** is closer to the oxygen atom and therefore exhibits a slightly stronger inductive effect, which accounts for the slightly shorter absorption and emission wavelengths of **SDX1**, compared to **SDX2**.

Then the spectral properties of **SDX3** and **SDX4** were studied. With the electron-donating amino group alkylated into a stronger diethylamino group, a bathochromic absorption and fluorescent emission spectra were anticipated. Unsurprisingly, **SDX4** showed a maximal absorbing wavelength at 410 nm in THF, exhibiting a notable bathochromic shift compared to the 380 nm of **SDX2**. Similar to **SDX1**/**2**, **SDX4** did not display a strong solvatochromism, and a slight bathochromic shift (ca. 10 nm) arose accompanied by an increase in solvent polarities from THF to DMSO. **SDX4** were strongly fluorescent with a maximal emitting wavelength at 495 nm in THF upon excitation at 410 nm and the fluorescent quantum yield was 0.53. With the solvent polarity increased, the maximal emitting wavelength of **SDX4** redshifted to 520 nm in DMSO with a high quantum yield of 0.84. However, the lone pair of electrons on nitrogen atom of the *ortho*-diethylamino group in **SDX3** couldn't effectively conjugate with the phenyl ring system due to the steric interaction. This decreased coplanarity weakened the electron donating capability of the second donor and the absorption of **SDX3** might exhibit a hypsochromic shift of ca. 50–60 nm, compared to **SDX4**. The maximal absorption wavelength of **SDX3** localized at ca. 360 nm in various solvent. The maximal emitting wavelength of **SDX3** was only ca. 20–30 nm shorter than **SDX4**. Therefore, a larger Stokes shift was observed for **SDX3** compared to **SDX4**.

Those four structurally-thrifty dyes (**SDX1/2/3/4**) exhibited diminished fluorescence emission in EtOH or H_2O (Tables 1 and S2), presumably due to hydrogen-bonding capability of the solvents to the carbonyl group of **SDX**s. For the same reason, the presence of trace water in these organic solvents will significantly lower the fluorescent quantum yields of those four dyes.

Based on this phenomenon, **SDX**s have potentials to be used as a microenvironment probe, to be fluorescent in non-hydrogen-bonding environment and non-fluorescent in hydrogen-bonding environment. To test our hypothesis, a surfactant was added into H_2O at a concentration higher than its critical micellar concentration (CMC) [33]. Specially, Tween-80 [34], a non-ionic surfactant, was used to prepare the micellar aqueous media with different weight fractions of Tween-80 from 0.5% to 10%. The fluorescence properties of **SDX4** in micellar media were investigated. **SDX4** was very weakly fluorescent in pure water (vide supra). In micellar aqueous media containing 10%, 5%, 2.5% and 1% Tween-80, a fluorescence enhancement of ca. 31-fold, 18-fold, 10-fold and 5-fold was observed, relative to the fluorescence intensity of **SDX4** in aqueous solution (Fig. 3). We postulated that **SDX4**, which are non-polar, prefers the non-polar and non-hydrogen-bonding environment of the micelles of Tween-80. This prevented the hydrogen-bonding between **SDX4** with water molecules and resulted in the fluorescent recovery of **SDX2**. This phenomenon demonstrated the potentials of **SDX2** in sensing the microenvironment associated with hydrogen-bond interaction and might find applications in monitoring biological functions involved with spatial conformations of protein and DNA helix [35].

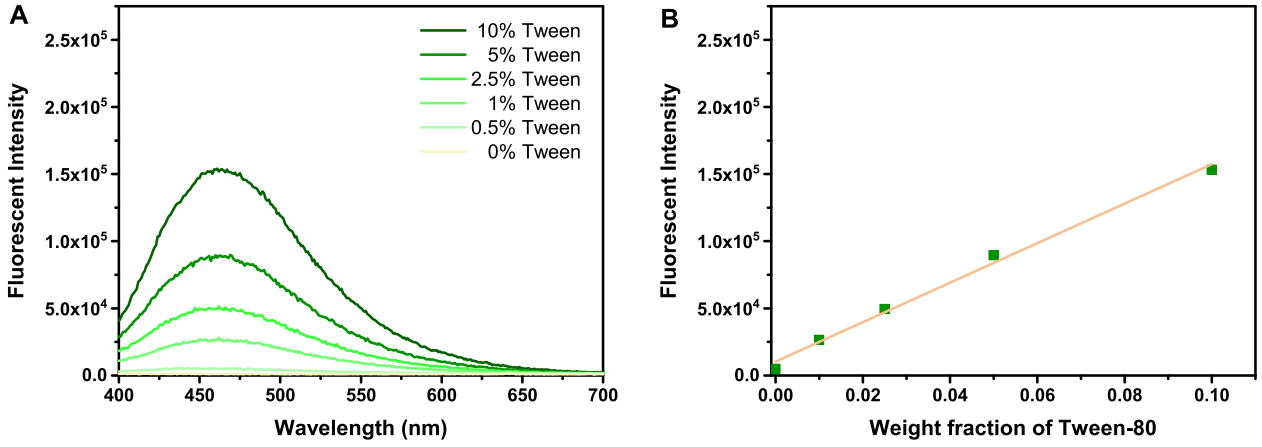

Fig. 3. (A) The fluorescent emission spectra of 10 μM **SDX4** in H_2O-Tween-80 mixtures measured with different weight fractions of Tween 80. (B) The plot of fluorescent intensity at 460 nm (λ_{ex} = 390 nm) versus the weight faction of Tween-80.

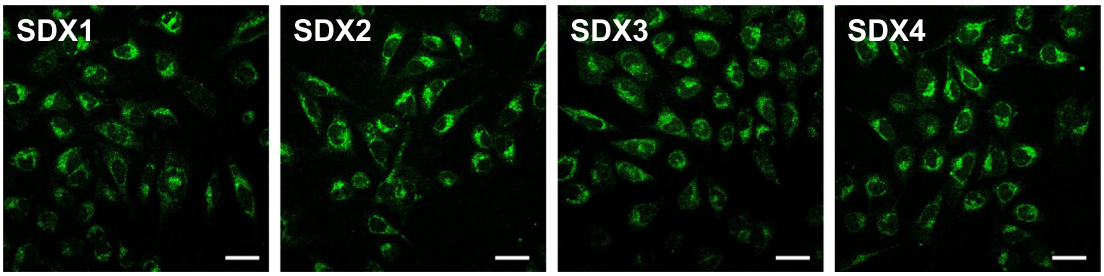

Fig. 4. Confocal images of BEAS-2B cells co-stained with 20 μM **SDX1/2/3/4**. (λ_{ex} = 405 nm, λ_{em} = 410–650 nm). Scale bar: 30 μm.

*3.3. Imaging of live cells incubated with **SDX**s*

The potentials of **SDX**s as live-cell imaging agents were examined with human lung epithelial BEAS-2B cell lines. **SDX**s showed good membrane permeability. They were essentially non-cytotoxic with a cell viability higher than 85% upon incubation of BEAS-2B cells with **SDX4** (up to 40 μM, Fig. S2). High signal-to-noise cell images were acquired with a confocal microscope (Fig. 4) and emissions of 410–650 nm were collected when a laser at 405 nm was used as excitation. This proves that **SDX**s have potentials for cell-imaging based applications.

4. Conclusions

In summary, a D′D-π-A principal was proposed for the design of structurally-thrifty and visible-absorbing fluorophores, and its viability was verified by the successful construction of **SDX**s. **SDX**s exhibited a strong green fluorescence emission with a quantum yield up to 0.84 and a large Stokes shift over 100 nm. **SDX**s were hydrogen-bonding sensitive, rendering them potentials for probing biological microenvironment associated with hydrogen-bond interaction. And the cell imaging capability of **SDX**s was demonstrated with BEAS-2B cells. The development of **SDX**s illustrated the effectivity of the D′D-π-A design strategy for constructing visible-absorbing/emitting fluorophores with minimum structures and provided valuable insight into the design of novel molecular probes.

CRediT authorship contribution statement

Xiao Luo: Investigation, Formal analysis, Writing - original draft, Funding acquisition. **Yan Chen:** Formal analysis. **Yanchun Li:** Formal analysis. **Zhenglong Sun:** Writing - review & editing. **Weihong Zhu:** Conceptualization, Writing - review & editing. **Xuhong Qian:** Conceptualization, Writing - review & editing. **Youjun Yang:** Conceptualization, Writing - review & editing, Funding acquisition.

Declaration of competing interest

The authors declare that they have no competing financial interests or personal relationships that could have appeared to influence the work reported in this paper.

Acknowledgement

The work is supported by the National Natural Science Foundation of China (Nos. 21822805 and 21908065), Shanghai Municipal Science and Technology Commission (No. 18DZ1112703) and China Postdoctoral Science Foundation (No. 2019M651427).

Appendix A. Supplementary data

Supplementary data to this article can be found online at https://doi.org/10.1016/j.saa.2020.118907.

References

[1] A.P. de Silva, H.Q.N. Gunaratne, T. Gunnlaugsson, et al., Signaling recognition events with fluorescent sensors and switches, Chem. Rev. 97 (1997) 1515–1566.
[2] L.D. Lavis, R.T. Raines, Bright ideas for chemical biology, ACS Chem. Biol. 3 (2008) 142–155.
[3] F. Deng, Z. Xu, Heteroatom-substituted rhodamine dyes: structure and spectroscopic properties, Chin. Chem. Lett. 30 (2019) 1667–1681.
[4] X. Bai, K.K. Ng, J.J. Hu, S. Ye, D. Yang, Small-molecule-based fluorescent sensors for selective detection of reactive oxygen species in biological systems, Annu. Rev. Biochem. 88 (2019) 605–633.
[5] J. Liu, W. Bu, J. Shi, Chemical design and synthesis of functionalized probes for imaging and treating tumor hypoxia, Chem. Rev. 117 (2017) 6160–6224.
[6] J.P. Celli, B.Q. Spring, I. Rizvi, et al., Imaging and photodynamic therapy: mechanisms, monitoring, and optimization, Chem. Rev. 110 (2010) 2795–2838.
[7] K.M. Dean, A.E. Palmer, Advances in fluorescence labeling strategies for dynamic cellular imaging, Nat. Chem. Biol. 10 (2014) 512–523.
[8] L. Wang, M.S. Frei, A. Salim, K. Johnsson, Small-molecule fluorescent probes for live-cell super-resolution microscopy, J. Am. Chem. Soc. 141 (2019) 2770–2781.
[9] E.A. Owens, M. Henary, G.E. Fakhri, H.S. Choi, Tissue-specific near-infrared fluorescence imaging, Acc. Chem. Res. 49 (2016) 1731–1740.
[10] C.C. Liu, P.G. Schultz, Adding new chemistries to the genetic code, Annu. Rev. Biochem. 79 (2010) 413–444.
[11] K. Lang, J.W. Chin, Cellular incorporation of unnatural amino acids and bioorthogonal labeling of proteins, Chem. Rev. 114 (2014) 4764–4806.
[12] X. Luo, Y. Yang, X. Qian, Recent progresses on the development of thioxonaphthalimides. Chin. Chem. Lett. 2020 https://doi.org/10.1016/j.cclet.2020.07.009
[13] W. Sheng, F. Lv, B. Tang, E. Hao, Lijuan Jiao, Toward the most versatile fluorophore: direct functionalization of BODIPY dyes via regioselective C–H bond activation, Chin. Chem. Lett. 30 (2019) 1825–1833.
[14] G.J. Clydesdale, G.W. Dandie, H.K. Muller, Ultraviolet light induced injury: immunological and inflammatory effects, Immunol. Cell Biol. 79 (2001) 547–568.
[15] J. Griffiths, Colour and Constitution of Organic Molecules, Academic Press, London, 1976.
[16] K. Mullen, G. Wegner, Electronic Materials: The Oligomer Approach, Wiley-VCH, Berlin, 1998.
[17] X. Luo, J. Li, J. Zhao, et al., A general approach to the design of high-performance near-infrared (NIR) D-π-A type fluorescent dyes, Chin. Chem. Lett. 30 (2019) 839–846.
[18] R.L.M. Allen, Colour Chemistry, 1st ed. Appleton-Century-Crofts, New York, 1971.
[19] E.V. Anslyn, D.A. Dougherty, Modern physical organic chemistry, University Science Books (2006) 65–145.
[20] M. Amaresh, M.K.R. Fischer, P. Bäuerle, Metal-free organic dyes for dye-sensitized solar cells: from structure: property relationships to design rules, Angew. Chem. Int. Ed. 48 (2009) 2474–2499.
[21] Y. Wu, W. Zhu, Organic sensitizers from D-π-A to D-A-π-A: effect of the internal electron-withdrawing units on molecular absorption, energy levels and photovoltaic performances, Chem. Soc. Rev. 42 (2013) 2039–2058.
[22] R.M. Christie, Why is indigo blue? Biotech. Histochem. 82 (2007) 51–56.
[23] J.S. de Melo, A.P. Moura, M.J. Melo, Photophysical and spectroscopic studies of indigo derivatives in their keto and leuco forms, J. Phys. Chem. A 108 (2004) 6975–6981.
[24] Y. Wang, H. Sun, L. Hou, et al., 1,4-Dihydroxyanthraquinone-Cu^{2+} ensemble probe for selective detection of sulfide anion in aqueous solution, Anal. Methods 5 (2013) 5493–5500.
[25] T. Beppu, K. Tomiguchi, A. Masuhara, Y.-J. Pu, H. Katagiri, Single benzene green fluorophore: solid-state emissive, watersoluble, and solvent- and ph-independent fluorescence with large stokes shifts, Angew. Chem. Int. Ed. 54 (2015) 7332–7335.
[26] B. Tang, C. Wang, Y. Wang, H. Zhang, Efficient red-emissive organic crystals with amplified spontaneous emissions based on a single benzene framework, Angew. Chem. 129 (2017) 12717–12721.
[27] B. Tang, H. Liu, F. Li, Y. Wang, H. Zhang, Single-benzene solid emitters with lasing properties based on aggregation-induced emissions, Chem. Commun. 52 (2016) 6577–6580.
[28] Y. Ning, Y. Huo, H. Xue, et al., Tri-manganese(III) salen-based cryptands: a metal cooperative antioxidant strategy that overcomes ischemic stroke damage in vivo, J. Am. Chem. Soc. 142 (2020) 10219–10227.

[29] H. Liu, S. Yan, R. Huang, Single-benzene-based solvatochromic chromophores: color-tunable and bright fluorescence in the solid and solution states, Chem. Eur. J. 25 (2019) 16732–16739.
[30] M.P. Hay, K.O. Hicks, K. Pchalek, H.H. Lee, A. Blaser, F.B. Pruijn, R.F. Anderson, S.S. Shinde, W.R. Wilson, W.A. Denny, Tricyclic [1,2,4]triazine 1,4-dioxides as hypoxia selective cytotoxins, J. Med. Chem. 51 (2008) 6853–6865.
[31] G.A. Crosby, J.N. Demas, Measurement of photoluminescence quantum yields. Review, J. Phys. Chem. 75 (1971) 991–1024.]
[32] G.A. Reynolds, K.H. Drexhage, New coumarin dyes with rigidized structure for flashlamp-pumped dye lasers, Opt. Commun. 13 (1975) 222–225].
[33] L.J.C. Love, J.G. Habarta, J.G. Dorsey, The micelle-analytical chemistry interface, Anal. Chem. 56 (1984) 1132–1144.
[34] M.E.D. Garcia, A. Sanz-Medel, Dye-surfactant interactions: a review, Talanta 33 (1986) 255–264.
[35] E.D. Glowacki, M. Irimia-Vladu, S. Bauer, N.S. Sariciftci, Hydrogen-bonds in molecular solids - from biological systems to organic electronics, J. Mater. Chem. B 1 (2013) 3742–3753.